3D-QSAR STUDY OF NEW ACETYL-COA:CHOLESTEROL
O-ACYL TRANSFERASE (ACAT) INHIBITORS[*]

Salvatore Guccione[1], Filippo Russo[1], and Thierry Langer[2]

[1] *Dipartimento di Scienze Farmaceutiche, Università di Catania,*
viale Andrea Doria 6, Ed. 12, I-95125 Catania, Italy
[2] *Institut für Pharmazie / Pharmazeutische Chemie, Leopold-Franzens-Universität Innsbruck*
Innrain 52a, A-6020 Innsbruck, Austria

Abstract - 3D QSAR models using comparative molecular field analysis (CoMFA) and comparative molecular similarity analysis (CoMSIA) were built on a training set of 19 previously described inhibitors of acetyl-CoA:cholesterol *O*-acyl transferase (ACAT) with a IC_{50} ranging from 47 nM to 200 µM. The models thus obtained were found to be predictive as shown by correct prediction of the inhibitory activity of a set of recently published compounds.

Introduction

Hypercolesterolemia has been identified as one of the major risk factors for coronary heart diseases. Many efforts have been directed towards the discovery of new and effective hypocolesterolemic drugs[1-3] . Acetyl-coA:cholesterol *O*-acyl transferase (ACAT) is a microsomal enzyme that catalyzes the formation of long chain fatty acid cholesterol esters[4,5]. It represents an attractive target to design novel hypolipidemic and anti-arteriosclerotic drugs since its inhibition produces a reduction in i) intestinal absorption of cholesterol, ii) liver secretion of very low density lipoprotein (VLDL) particles and iii) reduced accumulation of cholesterol esters in the arterial wall cells, the latter being a key step in the arteriosclerotic process[6-10]. Different types of ACAT inhibitors have been reported, however, an alkyl substituted urea or an amide group seem to be potential pharmacophores[11-13]. An exhaustive review has been presented by Matsuda[14]. Previously reported SAR and 3D-QSAR studies identified a message area represented by the diphenyl substituted heterocycle, responsible for the molecular recognition by the enzyme and a modulating area, which influences the activity through secondary *non covalent* interactions provided for by the heteroatomic parts of the molecule[11,15]. These features attracted our laboratories to test N-[(4,5-diphenyl)thiazol-2-yl]-N'-alkyl- or aryl ureas **20-34** and the corresponding thio derivatives **35-37**, combining the structural features of *anti*-ACAT compounds, for their biological activity[16]. The aim of the present work is to rationalize whether any such activity could be attributed to molecular shape and/or charge and H-

---

[*] *Dedicated with best personal wishes to Prof. Dr. Wolfgang Kubelka on the occasion of his 65th anniversary*

bond donor or acceptor function using two different 3D-QSAR approaches in order to address the synthesis of more potent ligands and to get insight into the unknown structure of the binding site of the target, acetyl-coA:cholesterol O-acyl transferase (ACAT).

Results and Discussion

CoMFA / CoMSIA

In order to develop quantitative structure activity relationships of the compounds under study we performed a 3D QSAR analysis using both the CoMFA[17] and the CoMSIA[18] approach. A training set of 19 previously described compounds[11] exhibiting an activity ranging from 47 nM to 200 μM was chosen. We are aware that the predictive capacity of a 3D QSAR model strongly depends on the structural variability of compounds used for model construction. The molecules presented in this study exhibit to a certain degree homology and therefore a CoMFA/CoMSIA derived from these compounds may not be predictive for ACAT inhibitors derived from other totally different structural classes. Our model, however, may represent an effective tool for the design of new diaryl imidazole or thiazole derivatives with pronounced ACAT inhibitory activity. The structures were aligned as shown in Fig. 1 by rigid body least-squares RMS fitting of all atoms of the central heteroaromatic moiety and subjected to CoMFA and CoMSIA. In order to determine how well the model predicts data, each predictive value was cross-validated using initially five components resulting in a determination of the optimum number of components. The results of the statistical evaluation is shown in Tab. 3 indicating that a satisfactory prediction can be obtained using three components. Moreover, in order to determine the stability of the model, the region was set to different offsets in X, Y, and Z direction and a correlation analysis was done for CoMFA, since it is well known that this method is highly sensitive towards slight changes of the position of the gridpoints around the molecules under investigation. All models exhibited a comparable predictivity, as expressed by r^2_{cv} in a range of 0.604 - 0.753 for CoMFA, and 0.747 – 0.803 for CoMSIA, respectively. A graphical representation of the bio-activity value prediction for the training set compounds is given in Fig. 2. Finally, PLS analysis of the descriptors generated from the initial region without cross-validation afforded the final model with a conventional r^2 of 0.940 (0.893) together with a standard error of estimate of 0.293 (0.381).

The standard deviation coefficient contour maps (Figures 3, 4, 5, 6, 7, and 8) derived from the final model display the 3D CoMFA / CoMSIA contributions of steric and electrostatic potentials, H-bond donor/acceptor functionality and lipophilicity. These contour maps indicate where the changes in fields are correlated with changes in binding affinity.

**Table 1.** Reference compounds used in the CoMFA / CoMSIA training set

Comp.	R	X
1	Ph	$C_{12}H_{25}$
2	Ph	
3	Ph	$CH(OEt)_2$
4	Ph	
5	Ph	
6	Ph	
7	Ph	
8	Ph	
9	Ph	$CH(OEt)_2$
10	Ph	
11	Ph	
12	Ph	
13	Ph	$CH(OMe)_2$
14	4-Me-Ph	
15	4-Cl-Ph	
16	4-MeO-Ph	
17	4-MeO-Ph	
18	4-Cl-Ph	
19	4-F-Ph	

Table 3. Statistical results of *CoMFA* and *CoMSIA* models

CoMFA Cross-validated analyses

field	field offset (Å)				S_{press}				
	x	y	z	r^2_{cv}	comp1	comp2	comp3	comp4	comp5
1	0	0	0	0.707	0.655	0.653	0.646	0.675	0.701
2	1	0	0	0.753	0.676	0.647	0.592	0.625	0.650
3	1	1	0	0.714	0.736	0.696	0.645	0.653	0.673
4	1	1	1	0.722	0.733	0.700	0.628	0.669	0.677
5	0	1	0	0.671	0.691	0.698	0.684	0.722	0.749
6	0	0	1	0.656	0.708	0.729	0.700	0.773	0.810
7	0	1	1	0.604	0.775	0.774	0.760	0.789	0.780

Final analysis without cross-validation (3 comp.)

| 1 | 0 | 0 | 0 | $r^2 = 0.940$ $s = 0.293$ $F_{(n_1=3, n_2=19)} = 109.276$ | | | | | |

CoMSIA Cross-validated analyses

field	r^2_{cv}	comp1	comp2	comp3
steric / electrostatic	0.747	0.585	0.586	0.600
H-bond acceptor / donor	0.789	0.523	0.539	0.565
hydrophobic	0.803	0.515	0.516	0.552
all fields together	0.792	0.524	0.531	0.552

Final analysis without cross-validation (3 comp.)

| all fields together | $r^2 = 0.893$ $s = 0.381$ $F_{(n_1=3, n_2=19)} = 91.784$ | | | |

Table 2. Predicted and measured IC_{50} of N-[(4,5-diphenyl)-thiazol-2-yl]-N'-alkyl- or aryl ureas **20-34** and thio derivatives **35-37**
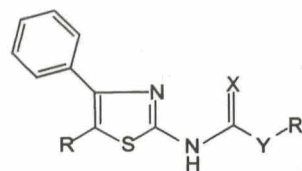

Compound	X	Y	R	R'	Measured IC_{50} (μM) [9]	CoMFA Predicted IC_{50} (μM)	CoMSIA Predicted IC_{50} (μM)
20	O	NH	C_6H_5	C_6H_5	80	45	39
21	O	NH	C_6H_5	2-FC_6H_4	200	45	45
22	O	NH	C_6H_5	2-MeO-C_6H_4	200	45	47
23	O	NH	C_6H_5	2,4-FC_6H_3	200	17	48
24	O	NH	C_6H_5	benzyl	200	32	41
25	O	NH	C_6H_5	cyclohexyl	10	23	39
26	O	NH	C_6H_5	C_3H_7	200	30	48
27	O	NH	C_6H_5	C_3H_7 (iso)	200	79	47
28	O	NH	C_6H_5	C_4H_9	5	26	48
39	O	NH	C_6H_5	C_7H_{15}	200	72	65
30	O	NH	C_6H_5	C_8H_{17}	200	76	69
31	O	NH	C_6H_5	$C_{12}H_{25}$	200	10	81
32	O	NH	H	C_4H_9	100	14	46
33	O	NH	H	cylohexyl	100	12	37
34	O	NH	H	C_6H_5	60	11	39
35	S	NH	C_6H_5	C_6H_5	200	17	21
36	S	NH	C_6H_5	benzyl	200	29	26
37	S	O	C_6H_5	C_4H_9	1000	16	10
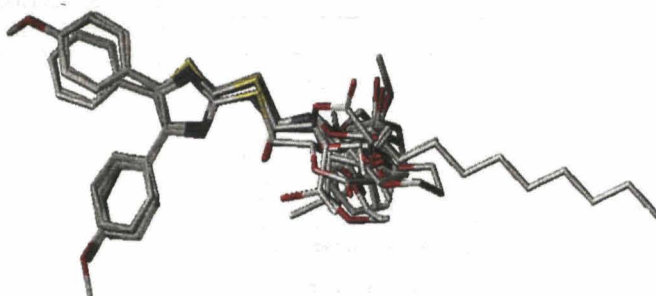
Figure 1: Alignment as used for the construction of the 3D-QSAR models

As can be deduced from the statistical parameters of the 3D QSAR analyses (r^2, r^2_{cv}, s_{press}), predictivity can be assumed for the model established within the class of compounds investigated. An advantage of such studies is the fact that conclusions concerning factors influencing
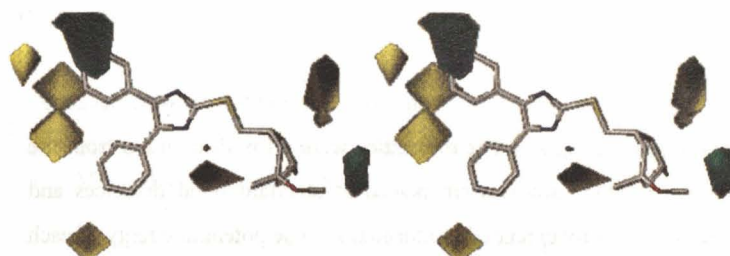
CoMFA

CoMSIA
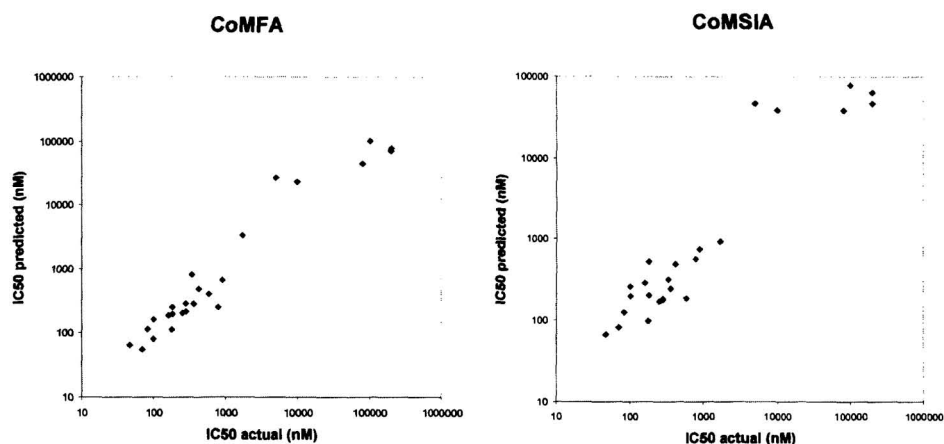
Figure 2: Actual and predicted IC_{50} (nM) values for training set compounds

the activity of a compound can be drawn directly from a correct interpretation of the interaction energy contour maps. From the CoMFA steric interaction contour map (Fig. 3) it can be deduced that the size of substituents at the phenyl rings is limited. This fact is in agreement with the observation that the 4-methoxy substituted derivatives (**16,17**) are less active than compounds bearing no substituent at the phenyl moiety. Also the length of the side chain is limited in a certain area (the methoxy group of the tetrahydropyran moiety in compound **4** would point into this region), whereas the model would suggest that a modest elongation in another area (green contoured zone in Fig. 3) could lead to compounds with enhanced activity. The interpretation of electrostatic energy interaction contour maps is more difficult. From Fig. 4 it may be deduced that enhancement of the positive charge in the area below and beside the heteroaromatic center of the molecules would lead to more active compounds. However, we are aware that conclusions drawn from electrostatic energy contour maps must be interpreted with care since calculations are always performed *in vacuo* and solvation effects are not taken into account. The CoMSIA contour plots are even more convenient for interpretation. In the CoMSIA steric contour plot (Fig. 5) one finds the same information than in the corresponding CoMFA graph, however, the image is less fragmented. From the CoMSIA electrostatic contour plot (Fig. 6) the negative effect of the electron rich C=O or C=S dipole for bio-activity in aryl ureas **20-34** and thio derivatives **35-37** is obvious. The H-bond acceptor effect of this group is also unfavourable for high activity as can be seen in Fig. 7, whereas the NH H-bond donor

function in the imidazole ring is indicated to contribute positively to bio-activity. As indicated by the magenta contour area in Fig. 7, H-bond accepting functions should also be present in the side chain. From the hydrophobicity field analysis (Fig. 8) it may be deduced that introduction of a group with high lipophilicity in the center of the molecule is preferable and that hydrophilic groups should be present in the side chain. Also in this plot, the positive effect of the imidazole NH function is outlined. Conclusively, the CoMSIA contour plots are found to be highly informative and easy to interpret.

Although some of the newly synthesized compounds were found to be less potent than predicted, the error of prediction lies in an acceptable range for 3D QSAR studies. Only for the thio derivatives **35-37**, the prediction capability of the model was found to be not satisfying. Apart from method inherent technical drawbacks, kinetic factors in the formation of the enzyme-inhibitor complex as a consequence of the isosteric oxygen-sulphur replacement may account for the *overestimation* by both of the computational methodologies used. The oxygen replacement with sulphur might be expected to be responsible for less favorable physicochemical characteristics such as solubility and hence negatively influence the bio-activity of this inhibitor chemotype. Conformational changes leading to an unfavourable spatial location of the pharmacophoric sub-structures or simply the bigger size of the sulphur atom when compared to the oxygen atom and the different reactivity of the carbonyl group *versus* the thione group[19] as hindering factors in accessing the active site might be also considered to explain the lack of activity in the thio derivatives **35-37**.

One suggestive mechanistic hypothesis is concerned with the decreased hydrogen bond accepting character of the thio derivatives **35-37**, also evidenced by the CoMSIA contour regions, which might affect the capability to disturb the hydrogen bond network acting as a gate for ligand entrance to the ACAT active site, so increasing the energy barrier associated for the formation of the enzyme-inhibitor complex. The gate opening ability of ACAT inhibitors by perturbing the network of hydrogen bonds at the entrance might be responsible for the access to the enzyme active site hence the inhibitor activity. Binding of the ligand disturbs the hydrogen bond network and it is consequently expected that the inhibitor forms a tight complex with the ACAT active site. The thio derivatives **35-37** might be impaired to perturb the hydrogen bond network and therefore the chances of the ligand to bind into the ACAT binding site are lower[20].

Figure 3: Relaxed stereoview of compound **10** in the *CoMFA* steric field contour graph. Contour levels shown correspond with contribution levels of standard deviation *x* coefficient of 80% and 20%, respectively (green: steric bulk favorable, yellow: steric bulk unfavorable)
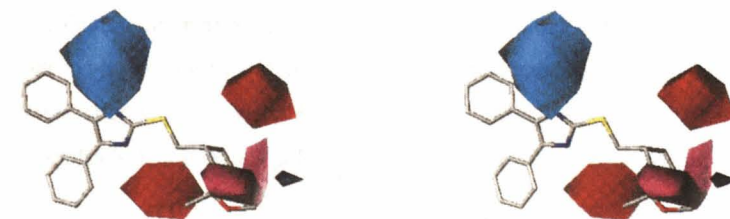
Figure 4: Relaxed stereoview of compound **10** in the *CoMFA* electrostatic field contour graph (blue: positive charge favorable; red: negative charge favorable).

Figure 5: Relaxed stereoview of compound **10** in the *CoMSIA* steric field contour graph (green: steric bulk favorable, yellow: steric bulk unfavorable)

Figure 6: Relaxed stereoview of compound **10** in the *CoMSIA* electrostatic field contour graph (blue: positive charge favorable; red: negative charge favorable).

Figure 7: Relaxed stereoview of compound **10** in the *CoMSIA* H-bond donor / acceptor field contour graph (cyan: H-bond donor favorable; purple: donor not favorable; magenta: H-bond acceptor favorable; red: acceptor defavorable).

Figure 8: Relaxed stereoview of compound **10** in the *CoMSIA* hydrophobic contour graph (yellow: hydrophobic area favorable; white: hydrophilic area favorable

Experimental Section

Molecular Modelling

The entire molecular modelling study was performed using the Sybyl 6.2 and 6.5 software package[21] running on Silicon Graphics desktop workstations. The molecules were all built de novo from the Tripos standard fragment library. Hydrogen atoms were placed at standard bond distances and angles. Flexible side-chains were set to a fully extended conformation. The potential energy of each structure was refined by a molecular mechanics procedure (MAXIMIN2 energy minimization procedure using the standard Tripos force field[22]) until the root mean energy gradient was less than 0.0005 kcal/mol Å. Partial atomic charges were calculated using the method of Gasteiger[23], and coulomb terms were included in the potential energy minimization process. CoMFA[17] and CoMSIA[18] was performed within the QSAR module of Sybyl. The requisite three-dimensional grid was generated automatically by the software (2 Å grid spacing in x, y, and z directions, box size 38x29x16 Å, 1800 data points) assuring that every grid in all directions protruded at least 4 Å beyond the shape of each molecule. Steric and electrostatic interaction energies at lattice intersections were generated with a probe atom that had the van der Waals properties of sp^3 carbon and a charge of +1.0. The steric and electrostatic energy values were truncated to 30 kcal/mol. The electrostatic energy term was ignored at lattice intersections yielding maximal (30 kcal/mol) steric values. In CoMSIA, the default value (0.3) for the attenuation factor was chosen. The linear expression of the CoMFA / CoMSIA results was calculated with the partial least-squares analysis (PLS)[24] algorithm in conjugation with the cross-validation procedure. This method provides a determination of the optimal number of components and permits an evaluation of predictivity of the model as indicated by the highest correlation (predictive r^2) value. PLS analysis of the descriptors with the same number of components but without cross-validation afforded conventional r^2 values.

References

1. Martin M. J., Hulley, S. B., Browner, W. S., Kuller, L. H., Wentworth, D. (1986) Lancet: 2, 933.
2. Badimon J. J., Fuster V., Chesebro J. H., Badimon L. (1993) Circulation: 87 (suppl. II), 3.
3. McCarthy, P. A. (1993) Med. Res. Rev.: 13, 139.
4. Spector A. A., Mathur S. N., Kaduce T. L. (1979) Prog. Lipid. Res.: 18, 31.
5. Suckling K. E., Stange E. F. (1985) J. Lipid. Res.: 26, 747.
6. Krause B. R., Anderson M., Bisgaier C. L., Bocan T., Bousley R., deHart P., Essenburg A., Hamelehle K., Homan R., Kieft K., McNally W., Stanfield R., Newton R.S. (1993) J. Lipid. Res.:34, 279.
7. Largis E. E., Wang C. H., DeVries V. G., Schaffer S. A. (1989) J. Lipid. Res.:30, 681.
8. Carr T. P., Rudel L. L. (1990) Arteriosclerosis: 10, 823.
9. Carr T. P., Parks J. S., Rudel L. L. (1992) Arterioscler. Thromb.: 12, 1274.
10. Gillies P. J., Robinson C. S., Rathgeb K. A. (1990) Arteriosclerosis: 12, 194.
11. Harris N. V., Smith C., Ashton M. J., Bridge A. W., Bush R. C., Coffee E. C. J., Dron D. I., Harper M. F., Lythgoe D. J., Newton C. G., Riddell D. (1992) J. Med. Chem.: 35, 4284 and references cited therein.
12. Sliskovic D. R., White A. D. (1991) Trends. Pharmacol. Sci.: 12, 194.
13. Tanaka A., Terasawa T., Hagihara H., Sakuma Y., Ishibe N., Sawada M., Takasugi H., and Tanaka H. (1998) J. Med. Chem.: 41, 2390.
14. Matsuda K. (1994) Med. Res. Rev.: 14, 271.
15. Mason J. S., McLay I. M., Lewis R. A. In New Perspectives in Drug Design, Dean P.M., Jolles J., Newton C.G. Eds. Academic Press, London (1995): pp 225.
16. Romeo G., Salerno L., Milla P., Siracusa M., Cattel L., Russo F., (1999) Pharmazie: 54,
17. Cramer III R. D., Patterson D. E., Bunce J. D. (1988) J. Am. Chem Soc.: 110, 5959.
18. Klebe G. In 3D QSAR in Drug Design, Kubinyi H., Folkers G., Martin Y. C. Eds. Kluwer Academic Publishers, Dordrecht (1998): pp 87-104.
19. Patai S., Rappopart Z. The Chemistry of Functional Groups, Supplement S: The Chemistry of Sulphur-containing Functional Groups, Chichester: John Wiley & Sons Ltd, Baffins Lane. (1993)
20. Llorens O., Perez J. J., Palomer A., Mauleon D. (1999) Bioorg. Med. Chem. Lett.: 9, 2779.
21. Sybyl, Tripos Associates, 1699 S. Hanley Road, Suite 303, St. Louis, MO63144, USA, 1995.
22. Clark M., Cramer III R. D., Van Opdenbosch N. J. (1989): Comput. Chem. 10, 982.
23. Gasteiger J., Marsili M. (1980) Tetrahedron: 36, 3219.
24. Wold S., Ruhe A., Wold H., Dunn W. J. (1984) SIAM J. Sci. Stat. Comp.: 5, 735.